# Linear stability analysis for a rotating cylinder with a rotating magnetic field

J. S. Walker
*Department of Mechanical and Industrial Engineering, University of Illinois, Urbana, Illinois 61801*

L. Martin Witkowski
*LIMSI, BP 133, F91403 Orsay Cedex, France*

(Received 30 September 2003; accepted 15 March 2004; published online 18 May 2004)

This paper treats the first hydrodynamic instability for a uniform-density, electrically conducting liquid in a finite-length cylinder which is rotating about its centerline. There is a uniform, transverse magnetic field which rotates about the cylinder's centerline and which produces a steady, axisymmetric, azimuthal body force on the liquid. For the initial transition from a steady, axisymmetric flow to a periodic, nonaxisymmetric flow, results for the critical value of the magnetic Taylor number and for the frequency of the critical disturbance are presented as functions of the Reynolds number for the cylinder rotation. Rotations of the cylinder and of the magnetic field in the same azimuthal direction and in opposite directions are considered. © *2004 American Institute of Physics.* [DOI: 10.1063/1.1737740]

## I. INTRODUCTION

A rotating magnetic field (RMF) can be used to stir an electrically conducting liquid. A RMF is produced by connecting the successive phases of a multiphase ac power source to a series of inductors at equally spaced azimuthal positions around an axis. A RMF has a spatially constant, transverse pattern which rotates with a constant angular velocity $\omega$ around its axis. For an electrically conducting liquid with azimuthal symmetry around the axis of the RMF, the periodic axial electric currents induced by the RMF interact with the RMF to produce an azimuthal body force on the liquid in the direction of the RMF rotation. This body force drives an azimuthal velocity in the liquid, and the axial variation of the centrifugal force due to this azimuthal velocity drives a meridional circulation with radial and axial velocities.

The application of a RMF during the continuous casting of steel or aluminum can produce more homogeneous castings with better metallurgical properties.[1] The metallurgical applications motivated the first models of the flow driven by a RMF.[2–4] A RMF was first applied during the growth of a single crystal from a body of molten semiconductor in 1958,[5] but major interest in the application of a RMF during semiconductor crystal growth did not begin until the 1990s. Dold and Benz[6] recently reviewed the experimental studies of semiconductor crystal growth with a RMF. Experiments have shown that the application of a RMF generally leads to a better crystal, as long as the flow driven by the RMF is steady and axisymmetric. Unfortunately an instability in the RMF-driven flow involves a transition to a periodic, nonaxisymmetric flow, and such a flow produces several undesirable properties in the crystal.

The first attempts to model the instability of the flow in a finite-length cylinder with a RMF involved the time-integration of the Navier–Stokes equations for unsteady, axisymmetric flow.[7–12] For a cylinder with a height to diameter ratio $b=1$, these studies predicted critical values of the magnetic Taylor number, $Tm_{cr}$, ranging from 54 000 to 280 000. This extreme disparity between the predictions of nominally equivalent numerical solutions was resolved by the linear stability analysis presented by Grants and Gerbeth.[13] Like the previous models, Grants and Gerbeth[13] only considered axisymmetric perturbations to the steady, axisymmetric base flow driven by a RMF in a finite-length cylinder. They demonstrated that extremely fine spatial resolution is required in order to obtain the correct result. They showed that there are three perturbation patterns which initially grow rapidly, but which ultimately decay, albeit very slowly. They also showed that small spatial truncation errors numerically amplify these perturbations enough to mask their true slow decay. For $b=1$, the correct $Tm_{cr}$ for the transition from the steady, axisymmetric base flow to a periodic axisymmetric flow is 163 610.[13] Grants and Gerbeth[14] recently presented a linear stability analysis with three-dimensional perturbations. They found that the first instability occurs at $Tm_{cr}=123\,200$ for $b=1$ and involves an $m=2$ mode, where $m$ is the integer azimuthal wave number.

A periodic, nonaxisymmetric flow during semiconductor crystal growth produces several undesirable characteristics in the crystal, so that a RMF should only be used with $Tm<Tm_{cr}$. The meridional circulation produced by a RMF is relatively small for $Tm<Tm_{cr}$, thus limiting the benefits from its stirring. It would be beneficial if the RMF-driven flow could be stabilized, leading to a larger meridional circulation before the instability of the steady, axisymmetric base flow. The addition of a rigid-body rotation stabilizes many flows, such as Rayleigh–Bénard convection.[15] For the current problem of flow in a finite-length cylinder with a RMF, a rigid-body rotation can be added by rotating the cylinder about its centerline. This situation differs from prob-

 

lems such as the Rayleigh–Bénard instability because here we are adding a rigid-body rotation to a flow which is already dominated by the azimuthal velocity. This paper represents an extension of the linear stability analysis presented by Grants and Gerbeth[14] since they considered a fixed cylinder and we consider a cylinder which is rotating either in the same direction as the RMF or in the opposite direction.

## II. PROBLEM FORMULATION

In addition to the primary periodic magnetic field produced by the inductors at equally spaced azimuthal positions around the liquid-filled cylinder, there is a secondary magnetic field which is produced by the periodic electric currents in the liquid and which partially cancels the primary magnetic field in the interior of the liquid. The significance of the secondary magnetic field depends on the value of the shielding parameter, $R_\omega=\mu\sigma\omega R^2$, where $\mu$ and $\sigma$ are the magnetic permeability and electrical conductivity of the liquid, while $R$ is the inside radius of the cylinder. In order to compute typical values of all dimensionless parameters, we use the properties of molten silicon[16] with $R=1$ cm and $\omega=100\pi$ rad/s (50 Hz). Our typical value for $R_\omega$ is 0.04, which is definitely so small that the secondary magnetic field is negligible.[17]

The RMFs for all crystal-growth experiments have involved uniform transverse magnetic fields. The electromagnetic (EM) body force produced by the RMF and the periodic electric currents in the liquid consists of: (1) a steady, axisymmetric, azimuthal body force, and (2) a periodic, nonaxisymmetric body force with a frequency of $2\omega$. If the frequency of the RMF is very low, e.g., 0.01 Hz, then the liquid responds to the periodic, nonaxisymmetric part of the EM body force, so that the flow is periodic and nonaxisymmetric for every value of the magnetic Taylor number.[18] For moderate frequencies, inertia limits the response to the periodic body force with frequency $2\omega$, so that the flow driven by the periodic, nonaxisymmetric part of the EM body force is negligible compared to the flow driven by the steady, axisymmetric part. The key parameters are the interaction parameter $N$ and the magnetic Taylor number $Tm$,

$$N=\frac{\sigma B^2}{\rho\omega}, \tag{1a}$$

$$Tm=\frac{\sigma\omega B^2R^4}{2\rho\nu^2}, \tag{1b}$$

where $\rho$ and $\nu$ are the density and kinematic viscosity of the liquid, while $B$ is the magnetic flux density of the RMF. For our typical example with silicon, $Tm=123\,200$ corresponds to $B=3.9$ mT, which gives $N=0.000\,019\,1$. The ratio of the maximum velocity driven by the periodic, nonaxisymmetric part of the EM body force to its steady, axisymmetric counterpart is at most $0.3N^{1/2}$ for $Tm$ around $10^5$, so that this ratio is at most 0.0013 for our typical example.[19] Thus we need only consider the steady, axisymmetric part of the EM body force produced by the RMF. In addition, the ratio of the maximum liquid velocity to $\omega R$ is $2.5N^{1/2}=0.011$, so that the liquid velocity can be neglected in Ohm's Law.[19] As a consequence, the periodic electric currents in the liquid and the EM body force due to the RMF are decoupled from the flow. Therefore this is not a magnetohydrodynamic flow with an intrinsic coupling between the EM variables and the velocity. Instead it is an ordinary hydrodynamic flow with a known, steady, axisymmetric, azimuthal body force.

We use cylindrical coordinates $(r,\theta,z)$ with the $z$ axis along the cylinder's centerline, which is also the axis of rotation of the RMF. We normalize $r$ and $z$ with $R$, so that the inside surfaces of the cylinder lie at $r=1$ and at $z=\pm b$. The dimensionless governing equations are

$$\frac{\partial\mathbf{v}}{\partial t}+(\mathbf{v}\cdot\nabla)\mathbf{v}=-\nabla p+Tmf_\theta\hat{\theta}+\nabla^2\mathbf{v}, \tag{2a}$$

$$\nabla\cdot\mathbf{v}=0, \tag{2b}$$

where $t$, $\mathbf{v}$, and $p$ are time, velocity, and pressure, normalized by $R^2/\nu$, $\nu/R$, and $\rho\nu^2/R^2$, respectively, while $f_\theta(r,z)$ is the dimensionless body force due to the RMF and $\hat{\mathbf{r}},\hat{\theta},\hat{\mathbf{z}}$ are unit vectors. For metallurgical applications, the solids at $z=\pm b$ are electrically conducting, so that $f_\theta=r$.[3,4] For crystal-growth applications, the solids at $z=\pm b$ have electrical conductivities which are much smaller than $\sigma$, so that

$$f_\theta=r-2\sum_{N=1}^{\infty}\frac{J_1(\lambda_N r)\cosh(\lambda_N z)}{(\lambda_N^2-1)J_1(\lambda_N)\cosh(\lambda_N b)}, \tag{3}$$

where $J_k$ is the Bessel function of the first kind and $k$th order, while $\lambda_N$ are the roots of $\lambda_N J_0(\lambda_N)-J_1(\lambda_N)=0$.[19] The boundary conditions are

$$\mathbf{v}=\mathrm{Re}_\Omega\,\hat{\theta}, \quad \text{at } r=1, \tag{4a}$$

$$\mathbf{v}=\mathrm{Re}_\Omega\, r\hat{\theta}, \quad \text{at } z=\pm b, \tag{4b}$$

where $\mathrm{Re}_\Omega=\Omega R^2/\nu$ is the Reynolds number for the cylinder rotation with angular velocity $\Omega$. Positive and negative values of $\mathrm{Re}_\Omega$ correspond to cylinder rotation in the same azimuthal direction as the RMF and in the opposite direction, respectively.

For each of the variables $v_r, v_\theta, v_z$, $p$, we introduce the form

$$v_r=v_{r0}(r,z)+\varepsilon\,\mathrm{Real}[v_{r1}(r,z)\exp(\lambda t-im\theta)]. \tag{5}$$

The subscript 0 denotes the variables for the steady, axisymmetric base flow, the subscript 1 denotes the complex modal functions, such as $v_{r1}=v_{r1R}+iv_{r1I}$, for the small, $O(\varepsilon)$ perturbation in the linear stability analysis, $\lambda=\lambda_R+i\lambda_I$ is the complex eigenvalue, and $m$ is the real, integer azimuthal wave number.

For the base flow, we introduce the stream function $\psi_0(r,z)$ for the meridional circulation, where

$$v_{r0}=\frac{1}{r}\frac{\partial\psi_0}{\partial z}, \tag{6a}$$

$$v_{z0}=-\frac{1}{r}\frac{\partial\psi_0}{\partial r}. \tag{6b}$$

We cross-differentiate the $r$ and $z$ components of the momentum equation (2a) for the steady, axisymmetric base flow in order to eliminate $p_0$. Since $\psi_0$ and $v_{\theta0}$ are odd and even

functions of $z$, respectively, we need only treat $0 \leqslant z \leqslant b$. We represent $\psi_0$ and $v_{\theta 0}$ by sums of products of Chebyshev polynomials in $r$ and $z$. In $z$, we use the polynomials with the correct symmetry. In $r$, we insure that each representation has the correct Taylor series in $r$, namely only odd powers of $r$ for $v_{\theta 0}$ and only even powers of $r$, starting with $r^2$, for $\psi_0$. We apply the governing equations and boundary conditions at the Gauss–Lobatto collocation points, including $r=0$ and $z=0$. For an equation or boundary condition which is odd in z, we apply its derivative at $z=0$. For example, the boundary condition $\psi_0(1,z)=0$ is applied at the Gauss–Lobatto collocation points, $z_K=\cos(K\pi/2NZ)$ for $K=1$ to $(NZ-1)$. Since $\psi_0$ is an odd function of $z$, it is automatically zero at $z=0$. Therefore we apply the additional boundary condition $\partial\psi_0/\partial z=0$ at $r=1$ and $z=0$. On the other hand, $v_{\theta 0}(1,z)=0$ is applied at every collocation point, including $z=0$, but $\partial v_{\theta 0}/\partial z$ is automatically zero at $r=1$ and $z=0$, by symmetry. Therefore each equation or boundary condition and its first derivative with respect to $z$ are both equal to zero at $z=0$. Since we want each equation or boundary condition to be as close to zero as possible between collocation points, applying the $z$ derivative at $z=0$ helps because the largest gap between collocation points is adjacent to $z=0$. For each equation or boundary condition, we introduce Taylor series in $r$, divide by the smallest power of $r$ and take the limit as $r\rightarrow 0$. We solve the nonlinear, algebraic equations for the coefficients in the Chebyshev polynomial representations using a Newton–Raphson iteration.

Since the base flow is symmetric in $z$, we need only treat $0 \leqslant z \leqslant b$ for the linear perturbation variables, as long as we consider both symmetric and antisymmetric modes. A symmetric mode has the same symmetry as the base flow, so that $v_{r1}, v_{\theta 1}$, and $p_1$ are even functions of $z$, while $v_{z1}$ is an odd function of $z$. For an antisymmetric mode, $v_{r1}, v_{\theta 1}$, and $p_1$ are odd functions of $z$, while $v_{z1}$ is an even function of $z$. Different formulations are required for axisymmetric perturbations with $m=0$ and nonaxisymmetric perturbations with $m \geqslant 1$. Therefore we must treat four cases: symmetric or antisymmetric modes with $m=0$ or $m \geqslant 1$. For axisymmetric modes with $m=0$, we introduce a perturbation stream function $\psi_1(r,z)$, which is related to $v_{r1}$ and $v_{z1}$ by Eqs. (6) with the subscript 0 replaced by the subscript 1. We eliminate $p_1$ by the same cross-differentiation, so that we have a fourth-order equation governing $\psi_1$ and a second-order equation governing $v_{\theta 1}$. For a nonaxisymmetric mode with $m \geqslant 1$, we eliminate $v_{\theta 1}$ with the continuity equation (2b) and we eliminate $p_1$ with the $\theta$ component of the momentum equation (2a). Each of these steps involves division by $m$. Thus we have two four-order equations governing $v_{r1}$ and $v_{z1}$. The pair of equations governing $v_{r1}$ and $v_{z1}$ represent a well-posed eigenvalue problem with (1) two boundary conditions on $v_{r1}$ and one boundary condition on $v_{z1}$ at $r=1$ and (2) one boundary condition on $v_{r1}$ and two boundary conditions on $v_{z1}$ at $z=1$. The extra boundary conditions come from $v_{\theta 1}=0$ which gives $\partial v_{r1}/\partial r=0$ at $r=1$ and $\partial v_{z1}/\partial z=0$ at $z=1$. Each perturbation variable is represented as a sum of products of Chebyshev polynomials with the correct symmetry in $z$ and with the correct Taylor series in $r$. For example, for $m \geqslant 1$, the Taylor series for $v_{r1}$ includes only the powers $r^{(m-1)}, r^{(m+1)}, r^{(m+3)}, r^{(m+5)}, \ldots$ . The linear equations and boundary conditions are applied at the Gauss–Lobatto collocation points, with the $z$-derivative of each odd equation applied at $z=0$ and with the first term in the Taylor series for each equation applied at $r=0$. The eigenvalues and eigenvectors are obtained with two different methods: (1) the shifted inverse iteration method[20] and (2) the rgg subroutine in the EISPAK library of eigenvalue subroutines. Inverse iteration is a very computationally efficient method to find the eigenvalue closest to a specified point in the complex $\lambda$ plane. Execution times for rgg are much longer than those for inverse iteration, but rgg gives all the eigenvalues. For the many runs needed to find individual points on the neutral stability curve, we primarily use inverse iteration, but we periodically repeat some calculations with rgg in order to insure that we are in fact focused on the critical mode. The rgg subroutine is particularly important near the transitions between azimuthal modes because it identifies the critical eigenvalue for the new value of $m$.

For specific values for $b$, $\mathrm{Re}_\Omega$ and $Tm$, we first use the Newton–Raphson iteration to find the steady, axisymmetric base flow, and then we use the inverse iteration method and rgg to find a number of eigenvalues for each of the symmetric and antisymmetric modes for $m=0,1,2,3,4,\ldots$ . For specific values of $b$ and $\mathrm{Re}_\Omega$, we increase $Tm$ until one eigenvalue for one mode has $\lambda_R=0$, while all other eigenvalues for this mode and for all other modes have $\lambda_R<0$. This defines the critical value of the magnetic Taylor number $Tm_{\mathrm{cr}}$, the dimensionless frequency $\lambda_I$, the azimuthal wave number $m$ and the symmetry in $z$ for the first instability for these values of $b$ and $\mathrm{Re}_\Omega$.

## III. RESULTS

Grants and Gerbeth[14] considered the variations of $Tm_{\mathrm{cr}}$ and $\lambda_I$ as functions of the aspect ratio $b$ for a fixed cylinder with $\mathrm{Re}_\Omega=0$. We consider the variations of $Tm_{\mathrm{cr}}$ and $\lambda_I$ as functions of $\mathrm{Re}_\Omega$ for a single aspect ratio $b=1$. Grid refinement studies indicated that 31 collocation points in $0 \leqslant r \leqslant 1$ and 47 collocation points in $0 \leqslant z \leqslant 1$ give accurate results for all of the cases considered here. For $b=1$ and $\mathrm{Re}_\Omega=0$, Grants and Gerbeth[14] found that the first instability involves a symmetric $m=2$ mode with $Tm_{\mathrm{cr}}=123\,200$ and $\lambda_I=160.42$, while we found the same mode with $Tm_{\mathrm{cr}}=123\,168$ and $\lambda_I=160.422$. Our calculations with several different grids indicate that the error in $Tm_{\mathrm{cr}}$ is less than 1% for $0 \leqslant \mathrm{Re}_\Omega \leqslant 1000$ with 31 radial and 49 axial collocation points. However, as $\mathrm{Re}_\Omega$ is decreased from zero, the numerical error for a fixed grid increases, apparently because the radial and axial gradients of $v_{\theta 0}$ near $r=z=1$ increase dramatically. For $\mathrm{Re}_\Omega=-225$, our calculations with several grids indicate that the error in $Tm_{\mathrm{cr}}$ is 2–3%. Clearly more collocations points would be needed for $\mathrm{Re}_\Omega<-225$, but we did not pursue this because negative values of $\mathrm{Re}_\Omega$ are clearly undesirable for crystal-growth applications. For all the cases considered here for $b=1$, the first instability involves a symmetric mode with $m=1$, 2, or 3.

The values of $Tm_{\mathrm{cr}}$ for $-225 \leqslant \mathrm{Re}_\Omega \leqslant 1000$ are presented in Fig. 1. As $\mathrm{Re}_\Omega$ is increased from zero, $Tm_{\mathrm{cr}}$ for the sym-

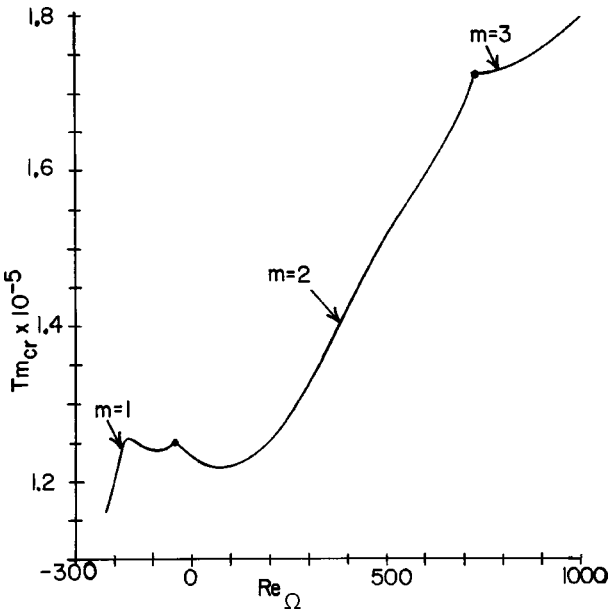


FIG. 1. Critical value of the magnetic Taylor number as a function of the Reynolds number for the cylinder rotation.

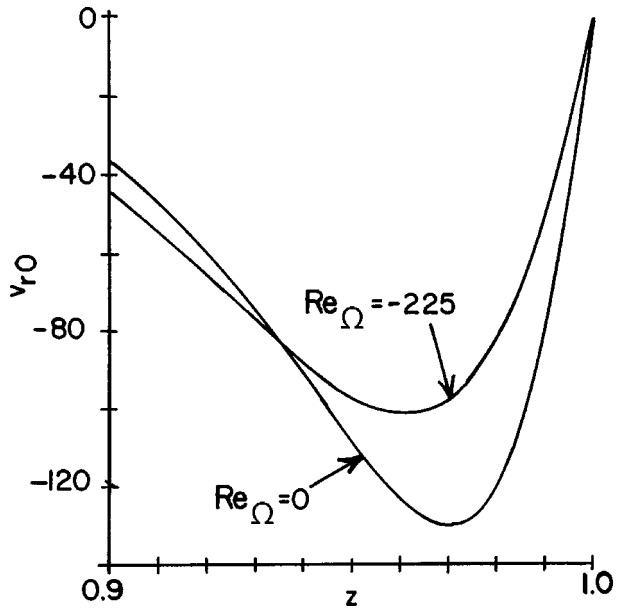


FIG. 2. Radial base-flow velocity vs $z$ at $r=0.9$ for $\mathrm{Re}_\Omega=0$ and $\mathrm{Re}_\Omega=-225$.

metric $m=2$ mode first decreases from 123 168 to 121 686 at $\mathrm{Re}_\Omega=80$ and then begins to increase. At $\mathrm{Re}_\Omega=728.46$ and $Tm_{\mathrm{cr}}=172319$, there is a switch from the symmetric $m=2$ mode to the symmetric $m=3$ mode. At $\mathrm{Re}_\Omega=1000$, $Tm_{\mathrm{cr}}=179610$. We have not gone beyond $\mathrm{Re}_\Omega=1000$ because this corresponds to 26.4 rpm for our typical silicon example, and crystal-growth systems are seldom rotated faster than 25 rpm. Clearly rotating the cylinder in the direction of the RMF can significantly increase the value of $Tm_{\mathrm{cr}}$. As $\mathrm{Re}_\Omega$ is decreased from zero, there is an increase of $Tm_{\mathrm{cr}}$ for the symmetric $m=2$ mode until the switch to the symmetric $m=1$ mode at $\mathrm{Re}_\Omega=-40$ and $Tm_{\mathrm{cr}}=125\,172$. For the symmetric $m=1$ mode, $Tm_{\mathrm{cr}}=127400$ for $\mathrm{Re}_\Omega=0$ and $b=1$.[14] As $\mathrm{Re}_\Omega$ is decreased from $-40$, there is a small increase in $Tm_{\mathrm{cr}}$ near $\mathrm{Re}_\Omega=-165$ and then $Tm_{\mathrm{cr}}$ begins to decrease rapidly. This rapid decrease of $Tm_{\mathrm{cr}}$ is apparently associated with the development of a region with $v_{\theta 0}<0$ near $z=1$. As $z$ is increased, the centrifugal force associated with $v_{\theta 0}$ decreases to zero along some surface below the top boundary and then increases again near the top. For much larger negative values of $\mathrm{Re}_\Omega$, this increasing centrifugal force near $z=1$ drives radially outward flow near $z=1$, but for $\mathrm{Re}_\Omega=-225$, its effect is simply to push the radially inward flow away from $z=1$. This is illustrated by the plots of $v_{r0}$ vs $z$ at $r=0.9$ for the critical modes for $\mathrm{Re}_\Omega=0$ and for $\mathrm{Re}_\Omega=-225$ in Fig. 2. The maximum values of $\psi_0$ are 14.497 and 14.492 for $\mathrm{Re}_\Omega=0$ and $\mathrm{Re}_\Omega=-225$, respectively, so that the magnitudes of the base-flow meridional circulations are almost equal, but at $r=0.9$, $v_{\theta 0}<0$ for $0.96\leqslant z\leqslant 1$ and for $\mathrm{Re}_\Omega=-225$, and this local centrifugal force pushes the inward part of the meridional circulation away from the top boundary. While the boundary layer is thicker for $\mathrm{Re}_\Omega=-225$, the local Reynolds number based on the minimum value of $v_{r0}$ and the distance of that minimum from $z=1$ is nearly the same for $\mathrm{Re}_\Omega=0$ and $\mathrm{Re}_\Omega=-225$.

There is a qualitative similarity between (1) the present flow with the RMF and cylinder rotating in opposite azimuthal directions and (2) the flow in a cylinder with its planar top and bottom boundaries rotating in opposite azimuthal directions. Gelfgat *et al.*[21] treated the transition from a steady, axisymmetric base flow to a periodic, axisymmetric flow for a cylinder with counter-rotating top and bottom. They presented the critical value of the Reynolds number based on the larger angular velocity, $\mathrm{Re}_{\mathrm{cr}}$, as a function of the ratio $\xi$ of the smaller angular velocity to the larger one. For $\xi=0$, $v_{\theta 0}\geqslant 0$ everywhere in the cylinder. As $\xi$ is decreased from zero, a region with $v_{\theta 0}<0$ begins to develop near the end counter-rotating with the smaller angular velocity. As $\xi$ is decreased from zero, Gelfgat *et al.*[21] found that $\mathrm{Re}_{\mathrm{cr}}$ first increases and then remains relatively constant until it decreases very rapidly from 2900 to 2000 near $\xi=-0.63$. The analogy between the present problem and the problem treated by Gelfgat *et al.*[21] is only qualitative for many reasons, but there appears to be a similarity between the rapid decrease of $Tm_{\mathrm{cr}}$ for $\mathrm{Re}_\Omega<-170$ in our problem and the rapid decrease of $\mathrm{Re}_{\mathrm{cr}}$ near $\xi=-0.63$ in their problem. Both rapid changes in stability appear to be related to the development of a region with $v_{\theta 0}<0$ which is large enough to significantly alter the characteristics of the meridional part of the base flow.

A critical perturbation for $m\geqslant 1$ has a constant spatial pattern which rotates in the $+\theta$ direction with a dimensionless angular velocity given by $\lambda_I/m$. The values of $\lambda_I/m$ for each critical mode for $-225\leqslant \mathrm{Re}_\Omega\leqslant 1000$ are plotted in Fig. 3. As noted by Grants and Gerbeth,[14] the $m=1$ mode propagates in the $-\theta$ direction. It is interesting that adding cylinder rotation in the $-\theta$ direction, which decreases the values of $v_{\theta 0}$ everywhere, reduces the magnitude of the negative angular velocity for the $m=1$ mode. At the transition from the $m=2$ symmetric mode to the $m=3$ symmetric mode, $\lambda_I/m$ jumps from 431.78 to 807.51. For all three modes, the critical perturbation is rotating with an angular velocity

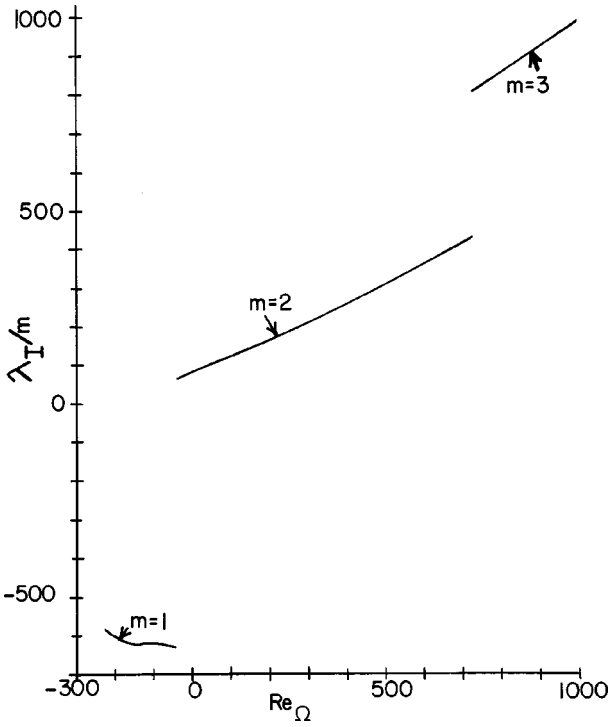


FIG. 3. Dimensionless azimuthal angular velocity $\lambda_I/m$ for the critical modes as a function of the Reynolds number for the cylinder rotation.

which is less than the average angular velocity of the base-flow azimuthal motion, so that some mechanism is causing the perturbation to lag behind the base-flow azimuthal motion. For the $m=1$ mode, this is clearly true because the perturbation propagates in the $-\theta$ direction while the average base-flow angular velocity is certainly positive even for $\mathrm{Re}_\Omega=-225$. Even for the $m=3$ mode, $\lambda_I/m$ is very close to $\mathrm{Re}_\Omega$, while $\mathrm{Re}_\Omega$ is the minimum dimensionless angular velocity for the azimuthal base flow, and the average is much larger.

Grants and Gerbeth[14] varied the aspect ratio $b$ of a fixed cylinder and found that the first instability involves a symmetric mode with $m=1$, 2, or 3 for different values of $b$. We have treated a rotating cylinder with a fixed aspect ratio $b=1$ and have found that the first instability involves a symmetric mode with $m=1$, 2, or 3 for different values of $\mathrm{Re}_\Omega$. Our plots of the magnitudes and phase shifts for $v_{r1}, v_{\theta 1}, v_{z1}$ for the critical modes with $m=1$, 2, or 3 closely resemble the corresponding plots presented by Grants and Gerbeth,[14] with the appropriate axial rescaling. Therefore we conclude that their explanations of the instability for each azimithal wave number are equally true for our results.

For crystal-growth applications, a disappointing result is that there is very little variation of the maximum value of $\psi_0$ at the critical magnetic Taylor number for $-225 \leqslant \mathrm{Re}_\Omega \leqslant 1000$. We have already noted that $\psi_{0\,\max}$ for $\mathrm{Re}_\Omega=-225$ is very close to $\psi_{0\,\max}$ for $\mathrm{Re}_\Omega=0$. For $\mathrm{Re}_\Omega<-170$, $\psi_{0\,\max}$ is decreasing as $\mathrm{Re}_\Omega$ is decreased and $Tm_{\mathrm{cr}}$ is decreasing rapidly. As $\mathrm{Re}_\Omega$ is increased from zero, $\psi_{0\,\max}$ first decreases from 14.497 to 14.118 at $\mathrm{Re}_\Omega=200$ and then increases to 14.750 at the transition from the symmetric $m=2$ mode to the symmetric $m=3$ mode at $\mathrm{Re}_\Omega=728.46$. However, after this transition, $\psi_{0\,\max}$ decreases with increasing $\mathrm{Re}_\Omega$, so that $\psi_{0\,\max}=14.243$ at $\mathrm{Re}_\Omega=1000$. Therefore rotating the cylinder in the same azimuthal direction as the RMF increases $Tm_{\mathrm{cr}}$, but it does not increase the maximum meridional circulation before transition to a periodic, nonaxisymmetic flow. The increase of $v_{\theta 0}$ everywhere as $\mathrm{Re}_\Omega$ is increased leads to a nearly constant meridional circulation in spite of the increase of $Tm_{\mathrm{cr}}$.

## IV. CONCLUSIONS

Rotating the ampoule or crucible during crystal growth with a RMF does not lead to an increase in the beneficial stirring before the undesirable transition to periodic, nonaxisymmetric flow. Rotation of the container in the azimuthal direction opposite to that of the RMF is definitely destabilizing. Rotation in the same direction increases the critical value of the magnetic Taylor number, but not the base-flow meridional circulation at the critical point.

## ACKNOWLEDGMENTS

Dr. I. Grants and Dr. G. Gerbeth of Forschungszentrum Rossendorf in Dresden shared eigenvalues for several modes over a range of values for $Tm$. This information was very valuable for the validation of our codes. This research was supported by the U.S. National Science Foundation under Grant No. CTS-0129028. The calculations were performed on a workstation donated by the International Business Machines Corporation.

[1] H. S. Marr, "Electromagnetic stirring in continuous casting of steel," in *Proceedings of the Symposium on Metallurgical Applications of Magnetohydrodynamics*, Cambridge, September 1982 (The Metals Society, London, 1984), p. 143.
[2] A. Alemany and R. Moreau, "Ecoulement d'un fluide conducteur de l'electricite en presence d'un champ magnetique tournant," J. Mec. **16**, 625 (1977).
[3] P. A. Davidson and J. C. R. Hunt, "Swirling recirculating flow in a liquid-metal column generated by a rotating magnetic field," J. Fluid Mech. **185**, 67 (1987).
[4] P. A. Davidson, "Swirling flow in an axisymmetric cavity of arbitrary profile, driven by a rotating magnetic field," J. Fluid Mech. **245**, 669 (1992).
[5] J. B. Mullin and K. F. Hulme, "On the use of electromagnetic stirring in zone refining," J. Electron. Control **4**, 170 (1958).
[6] P. Dold and K. W. Benz, "Rotating magnetic fields: Fluid flow and crystal growth applications," Prog. Cryst. Growth Charact. Mater. **38**, 7 (1999).
[7] Y. M. Gelfgat and L. A. Gorbunov, "Effects of alternating magnetic field on melt hydrodynamics in a cylindrical vessel with a free surface," Magnetohydrodynamics (N.Y.) **30**, 237 (1994).
[8] R. U. Barz, G. Gerbeth, U. Wunderwald, E. Buhrig, and Y. M. Gelfgat, "Modelling of the isothermal melt flow due to rotating magnetic fields in crystal growth," J. Cryst. Growth **180**, 410 (1997).
[9] T. Kaiser and K. W. Benz, "Taylor vortex instabilities induced by a rotating magnetic field: A numerical approach," Phys. Fluids **10**, 1104 (1998).
[10] J. Priede and Y. M. Gelfgat, "Numerical simulation of the MHD flow produced by a rotating magnetic field in a cylindrical cavity of finite length," Magnetohydrodynamics (N.Y.) **33**, 172 (1997).
[11] P. Marty, L. Martin Witkowski, P. Trombetta, T. Tomasino, and J. P. Garandet, "On the stability of rotating MHD flows," *Transfer Phenomena in Magnetohydrodynamic and Electroconducting Flows*, edited by A. Alemany, P. Marty, and J. P. Thibault (Kluwer, Dordrecht, 1999).
[12] R. Mößner and G. Gerbeth, "Buoyant melt flows under the influence of steady and rotating magnetic fields," J. Cryst. Growth **197**, 341 (1999).
[13] I. Grants and G. Gerbeth, "Stability of axially symmetric flow driven by a

rotating magnetic field in a cylindrical cavity,'' J. Fluid Mech. **431**, 407 (2001).
[14]I. Grants and G. Gerbeth, ''Linear three-dimensional instability of a magnetically driven rotating flow,'' J. Fluid Mech. **463**, 229 (2002).
[15]S. Chandrasekhar, *Hydrodynamic and Hydromagnetic Stability* (Dover, New York, 1961).
[16]P. Sabhapathy and M. E. Salcudean, ''Numerical study of Czochralski growth of silicon in an axisymmetric magnetic field,'' J. Cryst. Growth **113**, 164 (1991).
[17]L. Martin Witkowski, P. Marty, and J. S. Walker, ''Liquid-metal flow in a finite-length cylinder with a high-frequency rotating magnetic field,'' J. Fluid Mech. **436**, 131 (2001).
[18]J. S. Walker, ''Bridgman crystal growth with a strong, low-frequency rotating magnetic field,'' J. Cryst. Growth **192**, 318 (1998).
[19]L. Martin Witkowski, J. S. Walker, and P. Marty, ''Nonaxisymmetric flow in a finite-length cylinder with a rotating magnetic field,'' Phys. Fluids **11**, 1821 (1999).
[20]Y. Saad, *Numerical Methods for Large Eigenvalue Problems*, Manchester University Press Series in Algorithms and Architecture for Advanced Scientific Computing, 1991.
[21]A. Y. Gelfgat, P. Z. Bar-Yoseph, and A. Solan, ''Steady states and oscillatory instability of swirling flow in a cylinder with rotating top and bottom,'' Phys. Fluids **8**, 2614 (1996).